ISSN 2616-5767 Vol.9, Issue 3: 102-108, DOI: 10.25236/AJETS.2026.090314

Dynamic data modeling and simulation method of machine system based on grid finite element analysis

Li Huachuan[1,a,*], Huang Shangmeng[1,b]

[1]Department of Mechanical Engineering, Guangxi Technological College of Machinery and Electricity, Nanning, Guangxi, China
[a]35095758@qq.com, [b]87144560@qq.com
**Corresponding author*

Abstract: *The impact mechanical system of a new hydraulic power piling machine is researched and a dynamic data modeling and simulation method of mechanical system based on meshing finite element analysis is proposed. Based on a large number of research literatures on impact mechanical system dynamics at home and abroad, the finite volume method discrete equation is used and the Galerkin discrete finite element is adopted to approach it by mechanical elasticity equation to obtain the 3D unstructured mesh model of impact mechanical system of hydraulic power piling machine. The impact piling force of impact mechanical system of hydraulic power piling machine and meshing finite element of key parts are researched, including the punch hammer, tension and compression box, pull rod, pile caps etc. Finally, the LS-DYNA dynamics simulation software is used to simulate the finite elements for the impact mechanical system of hydraulic power piling machine. The results show the proposed method is effective.*

Keywords: *Meshing, Finite elements, Mechanical system, Modeling and simulation*

1. Introduction

Vibration, impact, acceleration and swing testers are core dynamic environmental test devices. Their complex coupled parameters, especially frequency characteristics, bring great design challenges. Traditional design relies on simplified analytical methods. For hydraulic vibration platform servo valves, conventional flow calculation neglects dynamic load fluctuations and adopts fixed load values. In actual operation, rising frequency reduces valve flow and aggravates phase lag, undermining system stability[1]. Such oversimplified approaches fail to accurately reflect dynamic system behaviors and induce latent design risks.

Simulation is a powerful approach for dynamic system analysis. It incorporates dynamic variables into differential equations to model system characteristics and acquire parametric time-domain responses. The advancement of full-digital simulation enables precise modeling of nonlinear links, greatly enhancing simulation fidelity. Driven by the popularization of microcomputers and simulation tools, simulation technology has been extensively applied in diverse industrial fields.

Simulation has undergone analog, hybrid and full-digital stages. The US analog computer invented in 1946 initiated analog simulation for aerospace motion simulation, thriving in the 1950s–1960s yet limited by low accuracy and poor controllability. Hybrid simulation emerged in the late 1950s and prevailed until the mid-1970s. The US AD10 full-digital simulator launched in 1978 ushered in the full-digital simulation era. In hydraulic simulation, HYDSIM, DSH and HASP were successively developed overseas. China's first full-digital simulator YH-F1 in 1985 marked its independent progress in full-digital simulation technology.

Initially limited to sophisticated aerospace system design, simulation has gained wide accessibility due to graphical programming tools. MATLAB/Simulink represents a critical technological breakthrough. Compared with traditional text-based modeling, it provides intuitive drag-and-drop graphical modeling and hierarchical architectures, supporting bidirectional top-down and bottom-up design. It clearly displays system internal coupling and data interaction, facilitating modeling and error calibration[2]. This tool adapts to various linear/nonlinear, continuous/discrete and multi-task systems. The milestone Simulink 6.5 significantly boosts computational efficiency via its acceleration algorithm.

Finite element, boundary element and finite volume methods are widely used in mechanical and

ISSN 2616-5767 Vol.9, Issue 3: 102-108, DOI: 10.25236/AJETS.2026.090314

fluid dynamic analysis, whereas stable discretization of nonlinear problems remains challenging. Current research adopts parameter stabilization and Nitsche penalty methods to optimize discrete solutions. This paper proposes a mesh-based finite element dynamic modeling and simulation method for the impact system of a novel hydraulic pile driver. LS-DYNA is employed for finite element simulation, and the results validate the feasibility and effectiveness of the proposed method.

2. Vibration Dynamic Model of Mechanical System of Piling Machine

In wave mechanics model, the pull rod and precast pile used in the impact mechanical system of hydraulic power piling machine is simplified as the elastic rod, where the transmission reflection of stress wave in pull rod is taken into consideration when the pull rod is simplified as the elastic rod, which makes the complex wave mechanics model and complicated solution procedure[3]. The vibration mechanics theory is used to simplify the pull rod as single spring-single mass block system and then the vibration mechanics model more simple and convenient than wave mechanics model can be built to obtain impact pilling force. As the complexity of mechanical model will not be increased if the precast pile is simplified as elastic rod, the precast pile is still assumed as elastic rod with equal wave drag in wave mechanics model.

According to the vibration mechanicals theory, the pull rod is simplified as the system composed of single mass unit and single spring unit (rigidity of pull rod), namely, the pull rod is simplified as a system with single degree of freedom. The pull rod mass unit is set as m4 (the mass is uniformly distributed on pile cap, tension and compression box) and the equivalent rigidity is set as k2. Other assumptions are same as wave mechanics model assumption. The structure of impact mechanical system of hydraulic power piling machine can be simplified as shown in Fig. 1.

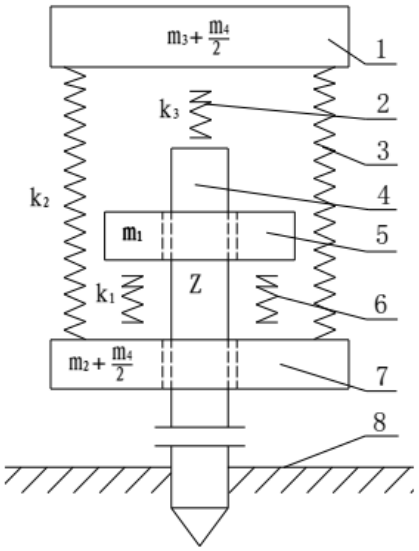

(1. Pile cap; 2. crash pad; 3. pull rod (spring); 4.central guide shaft 5. punch hammer; 6. buffer spring; 7. tension and compression box; 8. working medium

Fig. 1. Structure model of impact mechanical system of piling machine

3. Mechanical System Dynamics Modeling Based on Finite Element

3.1 Mesh structure discretization solutions

The geometrical elements are used to conduct mesh generation. In general, the tetrahedron is used to represent the substrate and the triangle element is used to represent the stress surface. The two-dimensional model mesh is used in order to simplify description as shown in Fig. 2. But in fact, the design method is three dimensional.

ISSN 2616-5767 Vol.9, Issue 3: 102-108, DOI: 10.25236/AJETS.2026.090314

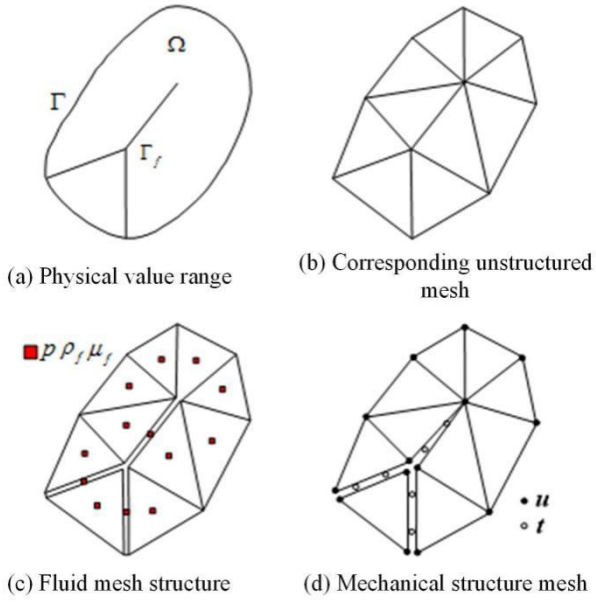

Fig. 2. Two-dimensional model mesh

In Fig. 2(a), Ω refers to the physical region, Γ refers to the outer shape of model and Γ_f is defined as stress surface. In Fig. 2b, the triangle is used to represent the substrate and the heavy line represents mechanical contact area. This geometry mesh is applicable to mechanical problems. In Fig. 2c, the control volume is associated with each element in mesh. Pressure p, density ρ_f and viscosity μ_f are all associated with cell center. The displacement is unknown and $\boldsymbol{u}$ is associated with top point of substrate. In Fig. 2d, different nodes are used to represent the displacement on each side in mechanical contact area. In addition, the traction vector $\boldsymbol{t}$ is associated with each mechanical contact area surface.

3.2 Mechanics equation and model approximation in discrete mechanical contact area

The stress equation of finite volume method is used to conduct discretization. Based on the approximate magnetic flow on two points, the flow rate between two adjacent controlled quantities can represent the pressure differential function:

$$Q_{ij} = \lambda T_{ij}(p_i - p_j) \tag{1}$$

Where, Q_{ij} is the mass flow rate between controlled quantity i and j. The dynamics fluidity can be defined as $\lambda = \rho_f / \mu_f$. The geometric transfer part is T_{ij}. The approximation scheme of finite volume of backward Euler time and flow rate is adopted and the flow rate equation (1) can be approximated as:

$$\frac{p_{fi}^{n+l}\phi_i^{n+1} - p_{fi}^{n}\phi_i^{n}}{\Delta t} V_i = \sum_j Q_{ij} + q_i v_i \tag{2}$$

Where, V_i is volume i and the time interval is Δt. The index $n+1$ and n respectively refer to the current and next step.

3.3 Quasi-static mechanical elasticity equation

Under the case of external boundary Γ and internal boundary Γ_f, the potential energy of mechanical contact defined in formula (2-3) can be further represented as:

$$\begin{aligned} \prod = & \frac{1}{2}\int_\Omega \boldsymbol{\varepsilon} : \boldsymbol{\sigma} d\Omega - \int_\Omega \boldsymbol{u}\rho\boldsymbol{g} d\Omega - \int_\Gamma \boldsymbol{u}\bar{\boldsymbol{t}} d\Gamma \\ & - \int_{\Gamma_f} \boldsymbol{u}^+ \bar{\boldsymbol{t}}_f^+ d\Gamma - \int_{\Gamma_f} \boldsymbol{u}^- \bar{\boldsymbol{t}}_f^- d\Gamma \end{aligned} \tag{3}$$

ISSN 2616-5767 Vol.9, Issue 3: 102-108, DOI: 10.25236/AJETS.2026.090314

Where, $\bar{\boldsymbol{t}}$ is the total traction vector on boundary Γ. The total traction force $\bar{\boldsymbol{t}}_f^-$ and $\bar{\boldsymbol{t}}_f^+$ are respectively in opposite side of fracture interface. Based on the continuity condition $\bar{\boldsymbol{t}}_f = \bar{\boldsymbol{t}}_f^+ = \bar{\boldsymbol{t}}_f^-$, it can be obtained that:

$$\begin{aligned}\prod = \frac{1}{2}\int_\Omega \boldsymbol{\varepsilon} : \boldsymbol{\sigma} d\Omega - \int_\Omega \boldsymbol{u}\rho\boldsymbol{g} d\Omega - \int_\Gamma \boldsymbol{u}\bar{\boldsymbol{t}} d\Gamma \\ - \int_{\Gamma_f} \left(\boldsymbol{u}^+ - \boldsymbol{u}^-\right)\bar{\boldsymbol{t}}_f \, d\Gamma\end{aligned} \tag{4}$$

Where, $\bar{\boldsymbol{t}}_f$ combines with the impact of mechanical pressure p and effective stress of Terzaghi $\boldsymbol{\sigma}'$.

$$\bar{\boldsymbol{t}}_f = -\boldsymbol{\sigma}\boldsymbol{n} = -(\boldsymbol{\sigma}' - \boldsymbol{I}p)\boldsymbol{n} = t_N\boldsymbol{n} + t_T\boldsymbol{\tau} + p\boldsymbol{n} \tag{5}$$

The gap function g can be expressed as the displacement function:

$$g = \boldsymbol{u}^+ - \boldsymbol{u}^- = (g_N, g_T) \tag{6}$$

Therefore, the following potential-energy function can be obtained:

$$\begin{aligned}\prod = \frac{1}{2}\int_\Omega \boldsymbol{\varepsilon} : \boldsymbol{\sigma} d\Omega - \int_\Omega \boldsymbol{u}\rho\boldsymbol{g} d\Omega - \int_\Gamma \boldsymbol{u}\bar{\boldsymbol{t}} d\Gamma \\ - \int_{\Gamma_f} g_N p d\Gamma - (\int_{\Gamma_f} g_N t_N + g_T t_T) d\Gamma\end{aligned} \tag{7}$$

The differential is used to calculate and obtain the minimum potential energy:

$$\begin{aligned}\delta\prod = \frac{1}{2}\int_\Omega \delta\boldsymbol{\varepsilon} : \boldsymbol{\sigma} d\Omega - \int_\Omega \delta\boldsymbol{u}\rho\boldsymbol{g} d\Omega - \int_\Gamma \delta\boldsymbol{u}\bar{\boldsymbol{t}} d\Gamma \\ - \int_{\Gamma_f} \delta g_N p d\Gamma - (\int_{\Gamma_f} \delta g_N t_N + \delta g_T t_T) d\Gamma = 0\end{aligned} \tag{8}$$

The finite element approximation can be made based on the node. Therefore, the displacement can be defined as:

$$\boldsymbol{u}(\xi) \approx \sum_a N_a(\xi)\boldsymbol{u}_a \tag{9}$$

Where, $\boldsymbol{u}_a$ is the node displacement value and N_a is the shape function. The gap function of impact mechanical system of hydraulic power piling machine can be defined as:

$$\begin{aligned}g(\xi) &= \boldsymbol{u}^+(\xi) - \boldsymbol{u}^-(\xi) \\ &\approx \sum_a N_a(\xi)(\boldsymbol{u}_a^+ - \boldsymbol{u}_a^-) = \sum_a N_a g_a\end{aligned} \tag{10}$$

Where, $\boldsymbol{u}^+$ and $\boldsymbol{u}^-$ respectively refer to the displacement on both sides of mechanical contact area. The surface discretization can be expressed as $\Gamma_f = \cup_e \Gamma_{f,e}$ and the stress area can be expressed as:

$$\begin{aligned}&\int_{\Gamma_f} \delta g_N p d\Gamma - \int_{\Gamma_f} (\delta g_N t_N + \delta g_T t_T) d\Gamma \\ &\approx \sum_e \times \int_{\Gamma_{f,e}} \sum_a \delta(g_N)_a N_a p d\Gamma \\ &- \sum_e \times \int_{\Gamma_{f,e}} (\sum_a \delta(g_N)_a N_a t_N + \sum_a \delta(g_T)_a N_a t_T) d\Gamma\end{aligned} \tag{11}$$

The traction vector (t_N, t_T) is shown above. Under the ideal condition, the friction law can be obtained based on Kuhn-Tucker relation:

$$\begin{cases} t_N \geq 0, g_N \geq 0, t_N g_N = 0, \dot{g}_T(\xi) - \eta \dfrac{\partial \Phi}{\partial t_T} = 0 \\ \Phi = \mid t_T \mid - \mathcal{F}(t_N) \leq 0, \eta \geq 0, \Phi \leq 0, \eta\Phi = 0 \end{cases} \tag{12}$$

It can be known that the slip phenomenon will occur when $\Phi = 0$; the adherence phenomenon will occur when $\Phi < 0$ and $\dot{g}_T = 0$. The Kuhn-Tucker constraint and adherence/slip rules can be replaced with:

ISSN 2616-5767 Vol.9, Issue 3: 102-108, DOI: 10.25236/AJETS.2026.090314

$$\begin{cases} \dot{g}_T(\xi) - \eta \dfrac{\partial}{\partial t_T} \Phi = \dfrac{1}{\varepsilon_T} \dot{t}_T \\ t_N = \varepsilon_N g_N, \eta \geq 0, \Phi \leq 0, \eta \Phi = 0 \end{cases} \tag{13}$$

Where, $\varepsilon_N \gg 1$, $\varepsilon_T \gg 1$ is penalty factor. ε_N is influence by man-made rigidity on stress surface. Based on the above formula, it can be known that the stress will occur when $g_N > 0$.

In deformation process, the contact area is directly proportional to the force imposed. Therefore, for the normal contact surface, the following formula is satisfied:

$$\mathcal{N}(g_N) = \frac{k_n g_0}{g_0 \cdot g_N} g_N \tag{14}$$

Where, k_n is the initial normal rigidity. Under the "ideal" condition, the surface roughness contact can be considered as below:

$$\begin{cases} t_N = \mathcal{N}(g_N), g_N \leq g_0 \\ \dot{g}_T - \eta \dfrac{\partial}{\partial t_T} \Phi = \dfrac{1}{\varepsilon_T} i_T \\ \eta \geq 0, \Phi \leq 0, \eta \Phi = 0 \end{cases} \tag{15}$$

The return mapping algorithm can be used to assess the traction vector as below:

$$\begin{cases} t_N^{n+1} = N(g_N^{n+1}) \\ t_T^{trial} = t_T^n + \varepsilon_T (g_T^{n+1} - g_T^n) \\ \Phi^{trial} = \mid t_T^{trial} \mid - \mathcal{F}(t_N^{n+1}) \\ t_T^{n+1} = t_T^{trial}, if\, \Phi^{trial} \leq 0 \\ \mid t_T^{n+1} \mid = \mathcal{F}(t_N^{n+1}), if\, \Phi^{trial} > 0 \end{cases} \tag{16}$$

Where, the subscript $n+1$ and n respectively refers to the current and previous step.

4. Experimental Analysis

4.1 Mesh model building

The hypermesh with powerful mesh generation function is selected to conduct mesh generation for the three-dimensional model of impact mechanical system. The good model will be built for the impact mechanical system of hydraulic power piling machine in Pro/E, the model is imported into Hypermesh, the surface mesh is firstly built for each part in Hypermesh, the high-precision hexahedral mesh can be obtained after tension and adjustment of surface mesh, where 3D solid element solid164 is used for the mesh element, the key part material and its overall model mesh are shown in Fig. 3a-d. Fig. 3a is the punch hammer mesh model, Fig. 3b is the tension and compression box mesh model, Fig. 3c is the local mesh model of pile cap and pull rod and Fig. 3d is the local mesh model of impact mechanical system. For the impact mechanical system model, the number of element is 89800 and the number of node is 124596.The material parameters of all core structural parts required for finite element calculation are summarized in Table 1. These material parameters including elastic modulus, Poisson's ratio and density are assigned to corresponding components during preprocessing.

Table 1: Material property of key parts

Name	Element type	Material	Elasticity modulus (Gpa)	Poisson ratio	Density (kg.mm/3)
Impact block	solid164	Steel	207GPa	0.28	7.83×10^{-6}
Tension and compression box	solid164	Steel	207GPa	0.28	7.83×10^{-6}
Pull rod	solid164	Steel	207GPa	0.28	7.83×10^{-6}
Pile cap	solid164	Steel	207GPa	0.28	7.83×10^{-6}
Precast pile	solid164	Concrete	30GPa	0.2	2.4×10^{-6}

ISSN 2616-5767 Vol.9, Issue 3: 102-108, DOI: 10.25236/AJETS.2026.090314

(a) Punch hammer

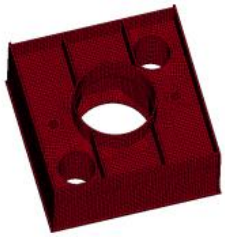

(b) Tension and compression box

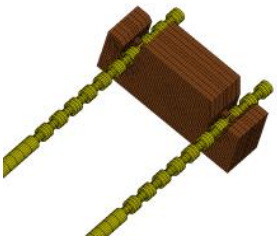

(c) Pile cap and pull rod

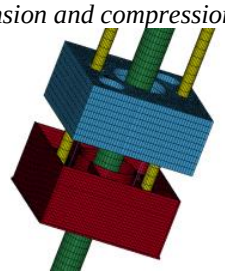

(d) Impact mechanical system

Fig. 3. Mesh model of key parts

The finite element mesh model of impact mechanical system of hydraulic power piling machine is imported into ANSYS to conduct pretreatment. The pretreatment process mainly includes the following steps:

(1) Establish part group: establish 7 part groups, namely, punch hammer, tension and compression box, pull rod, pile cap, pile, spring 1 and spring 2. Spring 1 is the spring rigidity between punch hammer and tension and compression box, namely, $k1 = 1 \times 10^9$N/m; spring 2 is the spring rigidity between pile cap and pile, namely, $k2 = 4 \times 10^8$N/m.

(2) Define the load and boundary conditions: add 6.12m/s of initial speed based on the design parameters of impact mechanical system of hydraulic power piling machine. We ignore the influences of soil layer on piling process in simulation and adopt full constraints at the bottom of precast pile.

(3) Establish the analysis options: set the computation time as 80ms, the output type as LS-DYNA and the output time interval as 0.2ms.

(4) Export setting: output the established simulation model in the format of K document; revise the contact and collision parameters etc. in the notebook and import the revised K document into LS-DYNASolver. As the impact process is transferred through spring, the automatic single face node-surface contact is adopted and the keyword is *CONTACT_AUTOMATIC_NODES_TO_SURFACE.

4.2 Impact piling force analysis

The contact surface element stress can be obtained from the finite element simulation results to calculate the piling force and compare with the theoretical value obtained above. Fig. 4a respectively represents the position of pile cap plane unit 45099 and the stress curve of such unit in axial direction (X direction) of precast pile. Fig. 4b represents the impact pile force curve under the theory of wave mechanics.

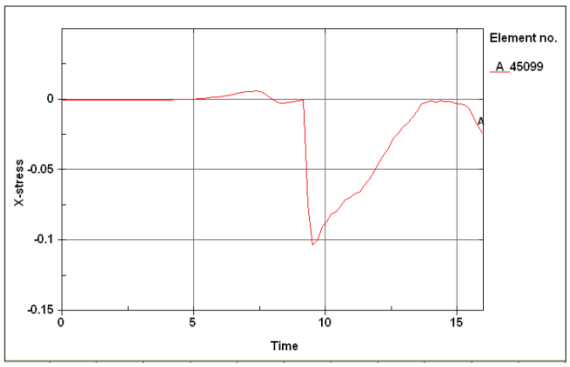

(a) The X direction stress curve of the unit 45099

ISSN 2616-5767 Vol.9, Issue 3: 102-108, DOI: 10.25236/AJETS.2026.090314

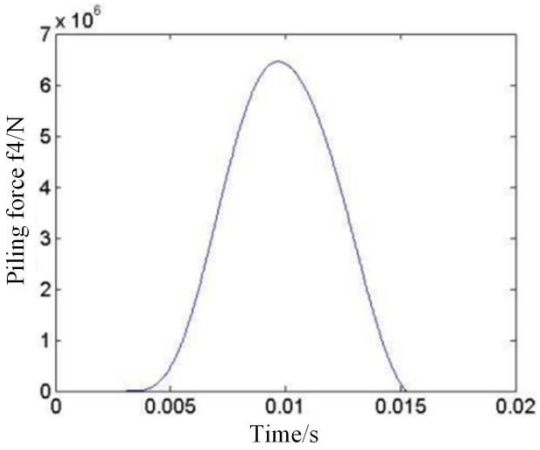

(b) The impact pile force curve under the theory of wave mechanics

Fig. 4. Impact pile force analysis

It can be known from Fig. 4a X-direction stress of unit 45099 is maximum at 9.5ms around. At this time, namely, in the simulation process, it is the occurrence time of maximum impact piling force. In Fig. 4b, the maximum impact piling force obtained under the theory appears in 0.01s, namely, 10ms around. By comparison with Fig. 4a and Fig. 4b, it can be known that the occurrence time of maximum impact piling force is basically consistent with the time of obtaining maximum impact piling force under the theory. However, in the theoretical results, the maximum impact piling force is 0.69×107N approximately, which is deviated from the result obtained through simulation. However, their occurrence time and variation tendency are basically similar. The structural features of each component have been taken into consideration in the simulation process. But the structural features are ignored in theoretical model. For example, the groove on top of pull rod, the clamping device between pile cap and pull rod and each rib plate on the tension and compression box are taken into consideration in simulation process; in the theoretical research, the pull rod is simplified as elastic rod with uniform section, but the rib plate structure in tension and compression box is ignored; the tension and compression box is simplified as a rigid body, these structural deviations will have an impact on transmission of stress wave in system and cause deviation between simulation results and theoretical results.

5. Conclusion

The impact mechanical system of a new hydraulic power piling machine is researched and a dynamic data modeling and simulation method of mechanical system based on meshing finite element analysis is proposed. Through LS-DYNA finite element analysis on the impact mechanical system of hydraulic power piling machine, it can be know that: (1) The LS-DYNA simulation curve and wave mechanicals theory calculation curve for impact piling force are basically similar, but the their maximum impact piling force is different. (2) From the hammer stress change cloud chart, it can be know that the stress is concentrated on the contact point of punch hammer and spring, the spring should be uniformly arranged or the crash pad can be used to replace the spring to reduce stress concentration of punch hammer.

References

[1] Miller K, Chinzei K, Orssengo G, et al. Mechanical properties of brain tissue in-vivo: experiment and computer simulation[J]. Journal of biomechanics, 2000, 33(11): 1369-1376.
[2] Felippa C A, Park K C, Farhat C. Partitioned analysis of coupled mechanical systems[J]. Computer methods in applied mechanics and engineering, 2001, 190(24): 3247-3270.
[3] Basdogan C, De S, Kim J, et al. Haptics in minimally invasive surgical simulation and training[J]. IEEE computer graphics and applications, 2004, 24(2): 56-64.